Available online at www.sciencedirect.com

ScienceDirect

journal homepage: www.elsevier.com/locate/nanoenergy
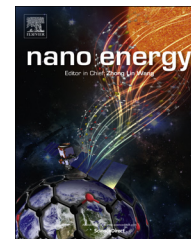
RAPID COMMUNICATION

Few-layered graphene quantum dots as efficient hole-extraction layer for high-performance polymer solar cells

Zicheng Ding[a], Zhen Hao[a], Bin Meng[a], Zhiyuan Xie[a], Jun Liu[a,*], Liming Dai[b,*]

[a]State Key Laboratory of Polymer Physics and Chemistry, Changchun Institute of Applied Chemistry, Chinese Academy of Sciences, Changchun 130022, PR China
[b]Department of Macromolecular Science and Engineering, Case School of Engineering, Case Western Reserve University, 10900 Euclid Avenue, Cleveland, OH 44106, USA

Abstract

In this study, we demonstrate that few-layered graphene quantum dots (F-GQDs) can be used as hole-extraction layer (HEL) for high efficiency polymer solar cells (PSCs). As a new class of HEL material, graphene oxide (GO) is not suitable for polymer solar cells (PSCs) based on highly efficient donor polymers due to the relatively low work function and the poor film-forming property of GO. To circumvent these two problems, we develop F-GQDs with a small size of about 4 nm and high content of periphery COOH groups. The small size of F-GQD ensures an excellent film-forming capability and the abundant COOH groups increase the work function of F-GQD to 5.26 eV from 5.01 eV of GO. As the result, when used as HEL in high efficiency PSC devices with $PTB7:PC_{71}BM$ or $PCDTBT:PC_{71}BM$ as the active layer, F-GQDs outperforms GO and the state-of-the-art HEL, PEDOT:PSS. These results demonstrate the great potential of F-GQD as efficient HELs to achieve high-performance PSCs.
© 2015 Published by Elsevier Ltd.

Introduction

Owing to their low cost, light weight, flexibility, and ever-increasing efficiency, polymer solar cells (PSC) have attracted great attention in the past two decades [1–5]. To improve power conversion efficiency (PCE) of PSCs, it is critical to facilitate charge extraction and prevent charge

*Corresponding authors.
  E-mail addresses: liujun@ciac.ac.cn (J. Liu),
liming.dai@case.edu (L. Dai).

recombination at the interfaces between the active layer and the cathode/anode electrodes. Therefore, a hole-extraction layer (HEL) between the anode and active layer and/or an electron-extraction layer (EEL) between the cathode and active layer are often required for high-performance PSCs [6-8]. However, the state-of-the-art HEL, poly(3,4-ethylenedioxythiophene) doped with poly (styrene sulfonate) (PEDOT:PSS), is still suffering from strong acidity and hygroscopicity to cause the device instability [9]. In order to maximize the PCE without the detrimental effect on device stability, several inorganic semiconductors, such as MoO_3, V_2O_5, NiO, WO_3 and RuO_2, have been used as the HEL in high-performance PSCs [10-14]. However, the use of these inorganic semiconductors increases the manufacturing cost as they need to be vacuum deposited. Recently, graphene oxide (GO) and its derivatives have emerged as a promising class of HEL materials with advantages of solution processability and low cost [15-24].

GO, a derivative of the one-atom-thick graphene with hydroxyl (OH) and epoxy groups on its basal plane and carboxyl groups (COOH) at the edge (see Scheme 1), often has a lateral size larger than several hundred nanometers and the work function of 4.7–5.0 eV [25,26]. Since the work function of GO matches well with the highest occupied molecule orbital (HOMO) level of the prototype donor polymer poly(3-hexylthiophene) (P3HT, HOMO: −4.9 eV) [20] for hole extraction, GO has been used as HEL in PSCs by several groups including our own one [15-19]. Due to the poor film-forming property intrinsically associated with the difficulties for large flakes of GO to uniformly cover the rough surface of indium-tin oxide (ITO) anode [16], the device performance of GO HEL cannot surpass that of PEDOT:PSS. Moreover, GO is not suitable for PSCs based on highly efficient donor polymers with deep HOMO levels ($< −5.1$ eV) [15,19]. The relatively low work function of GO induces an energy barrier for hole extraction and greatly decreases the PSC device efficiency. Therefore, solution-processable graphene materials with high work function and excellent film-forming property should be developed for high-efficiency PSC devices [21-24].

In this manuscript, we report the use of few-layered graphene quantum dots (F-GQD) with a small size of about 4 nm and high content of periphery COOH groups (see, Scheme 1) as excellent HEL in PSCs based on a highly efficient donor polymer, poly[[4,8-bis[(2-ethylhexyl)oxy]benzo[1,2-b:4,5-b′]dithiophene-2,6-diyl][3-fluoro-2-[(2-ethylhexyl) carbonyl]thieno[3,4-b]thiophenediyl]] (PTB7). The small size of F-GQD ensures an excellent film-forming capability [27,28] while the abundant COOH groups increase the work function

of F-GQD to 5.26 eV [29] from 5.01 eV of GO. The PSC device with PTB7 and [6,6]-phenyl-C71-butyric acid methyl ester ($PC_{71}BM$) as the active layer and F-GQD as the HEL is demonstrated to exhibit a PCE of 7.91%, outperforming its counterparts based on the GO (6.33%) and PEDOT:PSS (7.46%) HEL. To our best knowledge, the PCE thus achieved among the highest values reported for PSCs containing graphene materials [30-32].

Experimental section

Synthesis of GO

A mixture of graphite powder (1.00 g, 325 mesh), concentrated H_2SO_4 (25 mL), sodium nitrate (0.50 g) was stirred for 30 min in an ice-water bath and was slowly added $KMnO_4$ (4.50 g) under vigorously stirring, followed by stirring at 35 °C for 30 min and at 90 °C for another two hours. After cooled down, the mixture was slowly added into de-ionized water (100 mL) and H_2O_2 (30 mL). Centrifugation was carried out to precipitate the solid, which was washed with 1 M hydrochloric acid for three times and de-ionized water for another three times. The resultant solid was then dispersed in water by ultrasonication for 30 min, followed by centrifugation at 6000 rpm for 30 min. The supernatant was collected and purified through dialysis to afford aqueous GO solution (ca. 200 mL). To determine the concentration, 20 mL of the GO solution was filtered with a 0.22-μm membrane and then the dried in vacuum to give a solid content of 0.09 g. Hence, the concentration of the GO solution was 4.5 mg/mL and the yield of the reaction was 90%.

Synthesis of F-GQD

Vulcan VXC-72 carbon black (5.00 g, purchased from Cabot Corporation) was added into a mixture of concentrated H_2SO_4 (200 mL) and concentrated HNO_3 (100 mL). The mixture was stirred and refluxed for 24 h. After cooled down to room temperature, the mixture was at first neutralized with Na_2CO_3 powder and then acidified with hydrochloric acid to give pH=1. The resulting mixture was added into acetone (300 mL), followed by filtration to remove the precipitate. The filtrate was collected and the solvent was removed by rotary evaporation. The resulting deep yellow solid was dried in vacuum to afford F-GQD. Yield: 1.90 g, 38%.
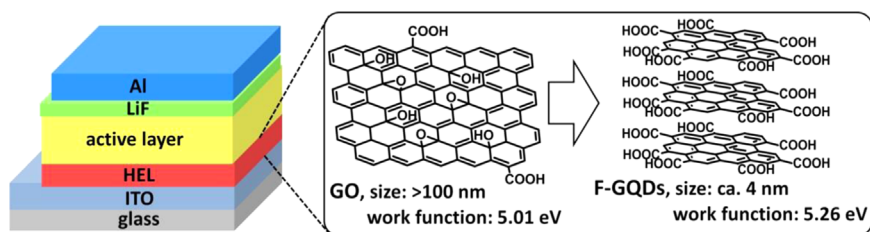
Scheme 1 (a) Device structure of the PSC. (b) Schematic structures of GO and F-GQD. Note the size and work function of GO and F-GQD underneath of the schematic structures.

PSC device fabrication and measurement

PTB7 (1-material Chemscitech Inc.) and PC$_{71}$BM (American Dye Source) were purchased from the commercial resources and used as received. poly[N-9″-hepta-decanyl-2,7-carbazolealt-5,5-(4′,7′-di-thienyl-2′,1′,3′-benzothiadiazole)] (PCDTBT) was synthesized in our laboratory. ITO glass substrates were ultrasonicated for 10 min each sequentially with detergent, de-ionized water, acetone, and iso-propanol, followed by drying at 120 °C overnight and UV-ozone treatment for 25 min. PEDOT:PSS (Baytron P VP A1 4083) was spin-coated on the pre-cleaned ITO substrate and baked at 120 °C for 30 min. The GO or F-GQD was spin-coated on the pre-cleaned ITO substrates from the aqueous solution with a concentration of 0.3 mg/mL, followed by annealing at 70 °C for 10 min. Then, all the substrates were transferred to a nitrogen-filled glove box. The PTB7:PC$_{71}$BM (1:1.5 by weight) active layer (100 nm) was spin-cast with the solution in chlorobenzene/1, 8-diiodoctane (97:3 by volume). The PCDTBT:PC$_{71}$BM (1:4 by weight) active layer (75 nm) was spin-coated from the dichlorobenzene solution. Finally, LiF (1 nm) and Al (100 nm) were sequentially deposited on the top of the active layer in a vacuum chamber with a pressure of about 4×10^{-4} Pa. The cell active area was 8 mm^2. Under illumination with the intensity of 100 mW/cm^2 provided by an Oriel 150 W solar simulator with an AM 1.5 G filter, J-V curves of the devices were measured using a Keithley 2400 source meter. The EQE was measured under the short-circuit condition with a lock-in amplifier (SR830, Stanford Research System) at a chopping frequency of 280 Hz during illumination with a monochromatic light from a Xenon lamp.

Results and discussion

F-GQD was synthesized by chemical oxidation of carbon black (Vulcan VXC-72, Cabot Corporation) in HNO$_3$/H$_2$SO$_4$ at gram scale following a modified literature method [33,34]. Since carbon black is the aggregates of spherical graphite particles with a diameter of about 30 nm, chemical oxidation of carbon black with strong acid readily affords F-GQD of even smaller lateral size. Compared with other solution approaches to synthesize graphene quantum dots from graphite, carbon nanotubes or fullerene, this approach from carbon black has advantages of scalability, high yield and low cost [33,34].

As shown in Figure 1, transmission electron microscopy (TEM, Figure 1a) reveals a uniform diameter of ca. 4 nm for F-GQD. The inset of image in Figure 1a shows that an in-plane lattice fringe of 0.208 nm, which may be reference to the (102) facets of sp^2 graphitic carbon [35]. The atomic force microscopic (AFM, Figure 1b) images shows that the thickness of F-GQD is about 2 nm. As single-layered graphene quantum dots or graphene oxide sheets have the thickness of 0.7-1 nm by AFM measurements, we estimated that F-GQD should contain two or three graphene layers [36,37]. The stacked graphene sheets in F-GQD may be attributed to the very low content of epoxy/hydroxy groups on the basal plane of the graphene sheets (vide infra).

The X-ray photoemission spectroscopy (XPS) survey spectrum shown in Figure 2a indicates that F-GQD (27.79 at.%)

contains a high content of oxygen species, similar to that of GO (29.27 at.%). The XPS C1s spectrum of F-GQD (Figure 2b) clearly shows the presence of C=C, C-C, C-O (hydroxy and epoxy), and COOH groups. Compared with GO, F-GQD possesses a much higher content of COOH groups and a significantly lower content of C-O groups, indicating that F-GQD contains a low content of epoxy/hydroxy groups on its basal planes and a high content of COOH groups at the edges, as schematically shown in Scheme 1. The high content of periphery COOH groups in F-GQD leads to good solubility in water and polar organic solvents, such as dimethylformamide (DMF), methanol, and acetone. Moreover, the F-GQD is insoluble in low-/non-polar organic solvents, such as chlorobenzene and o-dichlorobenzene, which are often used for spin-coating the active layer of PSCs. As such, F-GQD can be used as the underneath HEL free from being dissolved by the solvent used for solution-casting the active layer on top in the PSC (vide infra). Moreover, according to the theoretical calculation by Kumar et al., COOH groups can increase the work function of graphene oxide much more significantly than epoxy/hydroxy groups [29]. The high content of COOH groups in F-GQD is thus expected to result in a high work function, as seen below.

To verify the effect of chemical structure on work function of F-GQD and GO, we use ultraviolet photoelectron spectroscopy (UPS) to measure their work functions. The results are displayed in Figure 3b. According to the second electron cutoff in UPS spectra, the work functions of ITO, GO and F-GQD are estimated to be 4.80 eV, 5.01 eV and 5.26 eV, respectively. The higher work function of F-GQD than that of GO by 0.25 eV is attributed to the higher content of electron-deficient COOH groups in F-GQD (vide supra). The work function of F-GQDs is also higher than that of the graphene quantum dots (4.90 eV) reported by Chen et al., probably because of the smaller size (ca. 4 nm vs. 20-30 nm) and the higher content of periphery COOH groups in F-GQDs [27]. As shown in Figure 3c, with the increased work function, F-GQD can form Ohmic contact with the high-efficiency donor polymers, such as PTB7 [38] and PCDTBT [39], which can improve the hole extraction and suppress the electron/hole recombination on anode to afford a high photovoltaic efficiency.

In addition, F-GQD exhibits good film-forming property and high transparency in visible range, both are attractive for the HEL application. Figure 4 shows the AFM height images of F-GQD and GO films spin-coated on mica substrates from their 1 mg/mL aqueous solution. The F-GQD film is smooth and homogeneous with a root-mean-square (RMS) roughness of 0.14 nm and a peak-to-valley distance of 0.9 nm. No obvious voids can be observed in the AFM image of F-GQD film. In contrast, GO film is inhomogeneous with a RMS value of 0.73 nm and a peak-to-valley distance of 4.8 nm with various overlapped flakes and voids. For application of GO as HEL in PSCs, the overlapped flakes could suppress hole transport while the presence of voids would lead to direct contact of the anode and active layer [15] to reduce the device efficiency. The F-GQD with good film-forming capability can effectively avoid these problems associated with GO. Besides, the UV/Vis absorption spectrum of an aqueous solution of the F-GQD shows a peak at 225 nm with a shoulder at 355 nm and no absorption in
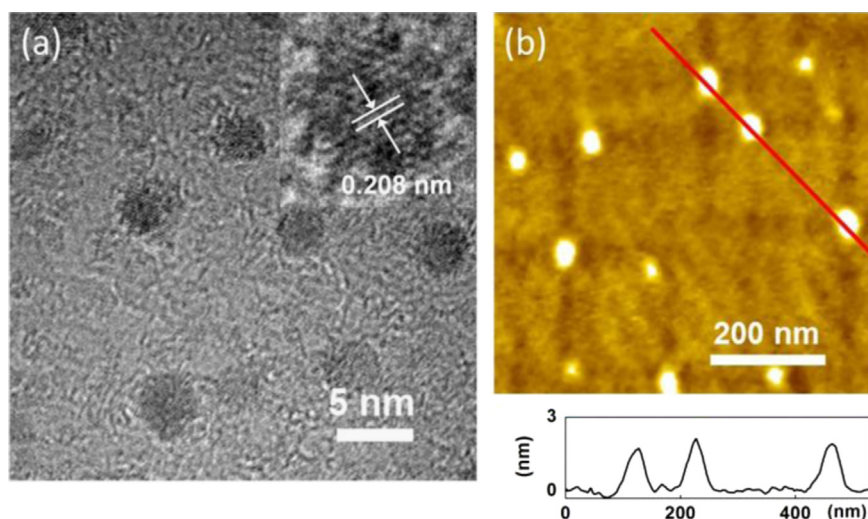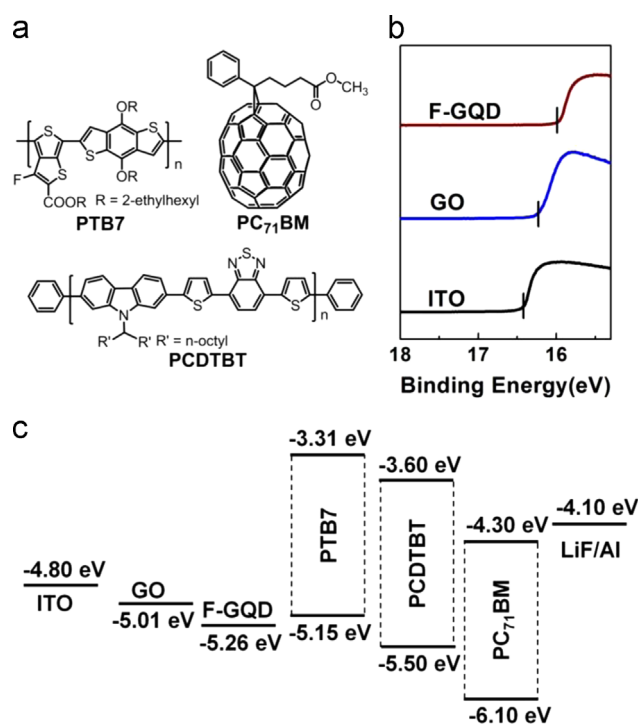
Figure 1 TEM image (a) and AFM height image (b) of F-GQD. The inset of (a) is a representative image of individual F-GQD. The bottom of (b) is the height profile corresponding to the line shown in the AFM image.
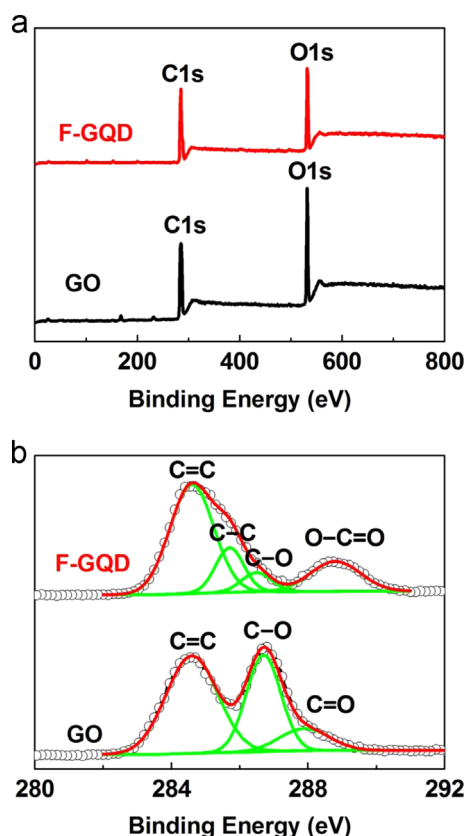

Figure 2 XPS survey spectra (a) and C1s spectra (b) of GO and F-GQD.

Figure 3 (a) Chemical structures of PTB7, PCDTBT and PC$_{71}$BM. (b) UPS spectra of ITO, GO and F-GQD. (c) Energy level alignment of the PSC devices with GO or F-GQD as HEL and PTB7 or PCDTBT as the donor polymer.

visible range (Figure S1). The F-GQD film spin-coated on an ITO glass is more transparent than PEDOT:PSS film in the region of 500-800 nm (Figure S3), allowing for more absorbance of solar light by the active layer in PSCs. The high work function, good film-forming capability, and high transparency of F-GQD prompt us to investigate the F-GQD as HEL for high-efficiency PSCs.

To evaluate the PSC device performance of the F-GQD HEL, we choose the benchmark highly efficient donor polymer, PTB7 [38], with HOMO of -5.15 eV. The device configuration is ITO/HEL/PTB7:PC$_{71}$BM (100 nm)/LiF (1 nm)/Al (100 nm) while HEL is none, PEDOT:PSS, GO or F-GQD. The chemical structures of PTB7 and PC$_{71}$BM are shown in Figure 3a. The current density–voltage (J-V) curves of the devices under simulated AM1.5 G illumination at 100 mW cm^{-2} are shown in Figure 5a and the corresponding parameters, including short-circuit current density (J_{SC}), open-circuit voltage (V_{OC}),
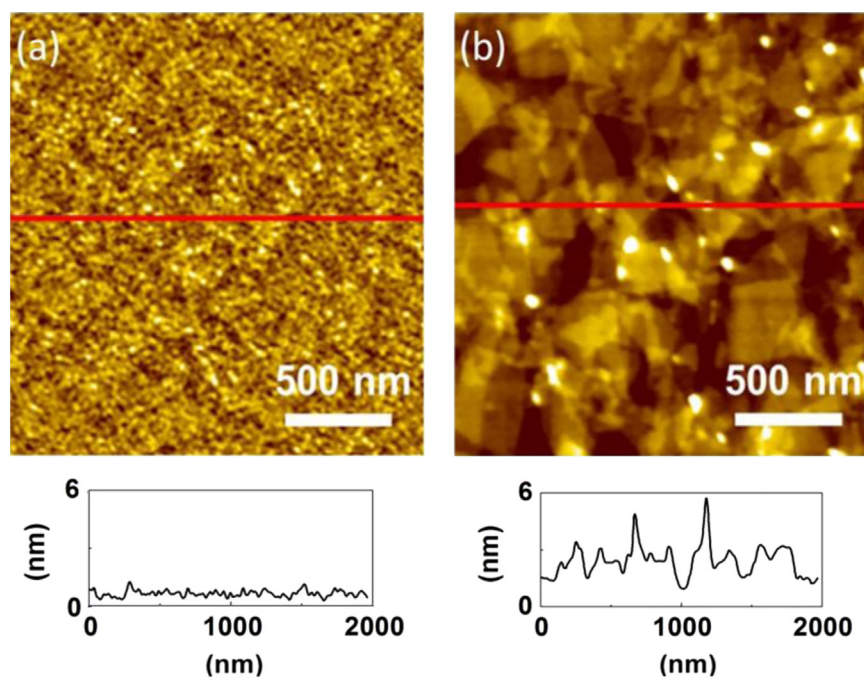
Figure 4 AFM height images of F-GQD film (a) and GO film (b) on mica substrates spin-coated from their 1 mg/mL aqueous solutions. The height profiles corresponding to the lines in the AFM images are also shown.
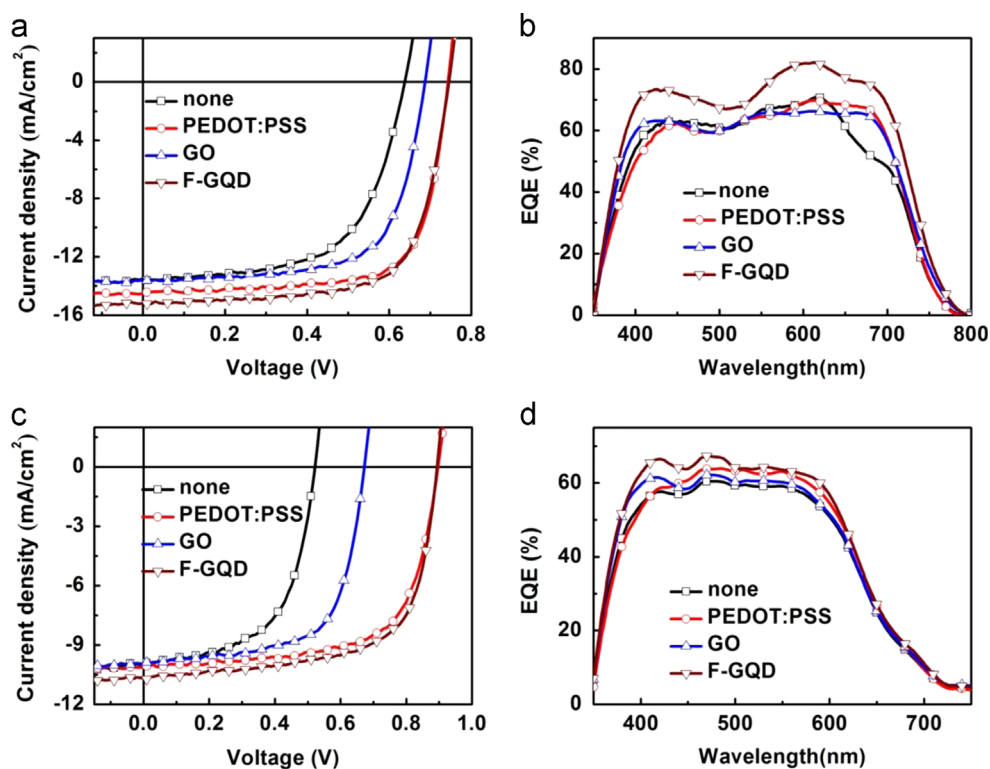
Figure 5 *J–V* curves (a) and EQE curves (b) of the devices based on PTB7 with different HELs. *J–V* curves (c) and EQE curves (d) of the devices based on PCDTBT with different HELs.

fill factor (FF) and PCE, are summarized in Table 1.The device with GO as HEL shows an V_{OC} of 0.69 V, J_{SC} of 13.58 mA/cm^2, FF of 0.68 and PCE of 6.33%. In comparison, the control device with PEDOT:PSS as HEL exhibits the V_{OC} of 0.74 V, J_{SC} of 13.96 mA/cm^2, FF of 0.72 and PCE of 7.46%.

The low V_{OC} of GO-based device is due to the non-Ohmic contact of the anode interface caused by the relatively low work function of GO (Figure 3b) [6-8]. In contrast, the F-GQD-based device shows the V_{OC} of 0.75 V, J_{SC} of 15.20 mA/cm^2, FF of 0.70 and PCE of 7.91%. The higher V_{OC} of the F-GQD-based

Table 1 Characteristics of the PSC devices based on PTB7 or PCDTBT with different HELs.

Donor	HEL	V_{OC} (V)	J_{SC} (mA/cm^2)	FF	PCE (%)
PTB7	None	0.64	13.51	0.61	5.27
	PEDOT:PSS	0.74	13.96	0.72	7.46
	GO	0.69	13.58	0.68	6.33
	F-GQD	0.75	15.20	0.69	7.91
PCDTBT	None	0.52	9.92	0.59	3.03
	PEDOT:PSS	0.90	10.11	0.66	6.02
	GO	0.67	9.97	0.65	4.34
	F-GQD	0.89	10.65	0.67	6.30

device than that of the GO-based device is attributable to the high work function of F-GQD, which leads to Ohmic contact. The major improvement of the F-GQD-based device compared to the PEDOT:PSS-based device comes from the increased J_{SC} from 13.96 to 15.20 mA/cm^2. The increased J_{SC} is consistent with the higher external quantum efficiency (EQE) of the F-GQD-based device than that of the PEDOT:PSS-based device (Figure 5b). F-GQD outperforms PEDOT:PSS due to the better transmittance of F-GQD than PEDOT:PSS (see Figure S3), which allows more solar light absorption by the active layer. Moreover, the good film-forming property of F-GQD is also crucial for its excellent PSC device performance.

The PSC device performance of F-GQD as HEL is further tested with PCDTBT:PC$_{71}$BM as the active layer. PCDTBT has an even deeper HOMO level of -5.50 eV and its chemical structure is shown in Figure 3a [39]. Figures 5c and d shows the J-V characteristics and the EQE curves, respectively, for the PSC devices with different HELs. Similar to the PSCs based on the PTB7:PC$_{71}$BM active layer, the PCDTBT:PC$_{71}$BM device with the GO HEL exhibits a low V_{oc} and low PCE due to the relatively low work function of GO. The corresponding device with F-GQD as HEL exhibits a V_{OC} of 0.89 V, J_{SC} of 10.65 mA/cm^2, FF of 0.67, and PCE of 6.30%, outperforming the counterpart with the PEDOT:PSS HEL (Table 1). Graphene quantum dots (GQDs) have been previously used as HEL in prototype P3HT-based PSCs [27], though with an inferior performance to PEDOT:PSS. In contrast, F-GQD with the unique structure (vide infra) is an excellent HEL superior to PEDOT:PSS, as demonstrated by the good device performance of F-GQDs in high-efficiency PSC devices investigated in this study.

Conclusions

In summary, we have developed F-GQD with a size of ca. 4 nm and abundant COOH groups as HEL materials for PSCs. Owing to its high work function, good film-forming property, and high transmittance, F-GQD HEL is demonstrated to show superior device performance than that of GO and PEDOT:PSS in PSCs based on high-efficiency donor polymers. The PSC with PTB7:PC$_{71}$BM as the active layer and F-GQD as the HEL exhibits a PCE of 7.91%, which is among the highest values reported for PSCs based on graphene materials. This work represents a major advance toward the practical application of solution-processable graphene materials in high-performance PSCs.

Acknowledgments

Appendix A. Supporting information

Supplementary data associated with this article can be found in the online version at http://dx.doi.org/10.1016/j.nanoen.2015.04.019.

References

[1] G. Yu, J. Gao, J.C. Hummelen, F. Wudl, A.J. Heeger, Science 270 (1995) 1789-1791.
[2] G. Li, R. Zhu, Y. Yang, Nat. Photonics 6 (2012) 153-161.
[3] K.H. Hendriks, G.H.L. Heintges, V.S. Gevaerts, M.M. Wienk R.A.J. Janssen, Angew. Chem. Int. Ed. 52 (2013) 8341-8344.
[4] H.X. Zhou, L.Q. Yang, S.C. Price, K.J. Knight, W. You, Angew. Chem. Int. Ed. 49 (2010) 7992-7995.
[5] B.C. Thompson, J.M.J. Frechet, Angew. Chem. Int. Ed. 47 (2008) 58-77.
[6] L.M. Chen, Z. Xu, Z.R. Hong, Y. Yang, J. Mater. Chem. 20 (2010) 2575-2598.
[7] R. Steim, F.R. Kogler, C.J. Brabec, J. Mater. Chem. 20 (2010) 2499-2512.
[8] H.-L. Yip, A.K.-Y. Jen, Energy Environ. Sci. 5 (2012) 5994-6011.
[9] Y.H. Kim, S.H. Lee, J. Noh, S.H. Han, Thin Solid Films 510 (2006) 305-310.
[10] V. Shrotriya, G. Li, Y. Yao, C.W. Chu, Y. Yang, Appl. Phys. Lett. 88 (2006) 073508.
[11] J.J. Jasieniak, J. Seifter, J. Jo, T. Mates, A.J. Heeger, Adv. Funct. Mater. 22 (2012) 2594-2605.
[12] M.D. Irwin, B. Buchholz, A.W. Hains, R.P.H. Chang, T.J. Marks, Proc. Natl. Acad. Sci. USA 105 (2008) 2783-2787.
[13] M.Y. Chan, C.S. Lee, S.L. Lai, M.K. Fung, F.L. Wong, H.Y. Sun, K.M. Lau, S.T. Lee, J. Appl. Phys. 100 (2006) 094506.
[14] B.P. Rand, J. Li, J.G. Xue, R.J. Holmes, M.E. Thompson S.R. Forrest, Adv. Mater. 17 (2005) 2714-2718.
[15] J. Liu, M. Durstock, L. Dai, Energy Environ. Sci. 7 (2014) 1297-1306.
[16] J. Liu, Y.H. Xue, Y.X. Gao, D.S. Yu, M. Durstock, L.M. Dai, Adv. Mater. 24 (2012) 2228-2233.
[17] J. Liu, G.-H. Kim, Y. Xue, J.Y. Kim, J.-B. Baek, M. Durstock, a. L. Dai, Adv. Mater. 26 (2014) 786-790.
[18] J. Liu, Y.H. Xue, L.M. Dai, J. Phys. Chem. Lett. 3 (2012) 1928-1933.
[19] Y.H. Chen, W.C. Lin, J. Liu, L.M. Dai, Nano Lett. 14 (2014) 1467-1471.
[20] S.S. Li, K.H. Tu, C.C. Lin, C.W. Chen, M. Chhowalla, Acs Nano 4 (2010) 3169-3174.
[21] Y. Gao, H.L. Yip, K.S. Chen, K.M. O'Malley, O. Acton, Y. Sun, G. Ting, H.Z. Chen, A.K.Y. Jen, Adv. Mater. 23 (2011) 1903-1908.
[22] D. Yang, L. Zhou, W. Yu, J. Zhang, C. Li, Adv. Energy Mater. 4 (2014) 1400591.
[23] J.M. Yun, J.S. Yeo, J. Kim, H.G. Jeong, D.Y. Kim, Y.J. Noh S.S. Kim, B.C. Ku, S.I. Na, Adv. Mater. 23 (2011) 4923-4928.

[24] Y.-H. Chao, J.-S. Wu, C.-E. Wu, J.-F. Jheng, C.-L. Wang C.-S. Hsu, Adv. Energy Mater. 3 (2013) 1279-1285.

[25] G. Eda, M. Chhowalla, Adv. Mater. 22 (2010) 2392-2415.

[26] D.R. Dreyer, S. Park, C.W. Bielawski, R.S. Ruoff, Chem. Soc. Rev. 39 (2010) 228-240.

[27] M. Li, W. Ni, B. Kan, X. Wan, L. Zhang, Q. Zhang, G. Long, Y. Zuo, Y. Chen, Phys. Chem. Chem. Phys. 15 (2013) 18973-18978.

[28] H.B. Yang, Y.Q. Dong, X.Z. Wang, S.Y. Khoo, B. Liu, ACS Appl. Mater. Interfaces 6 (2014) 1092-1099.

[29] P.V. Kumar, M. Bernardi, J.C. Grossman, ACS Nano 7 (2013) 1638-1645.

[30] J.K. Kim, M.J. Park, S.J. Kim, D.H. Wang, S.P. Cho, S. Bae J.H. Park, B.H. Hong, ACS Nano 7 (2013) 7207-7212.

[31] Y. Li, Y. Hu, Y. Zhao, G.Q. Shi, L.E. Deng, Y.B. Hou, L.T. Qu, Adv. Mater. 23 (2011) 776-780.

[32] I.P. Murray, S.J. Lou, L.J. Cote, S. Loser, C.J. Kadleck, T. Xu J.M. Szarko, B.S. Rolczynski, J.E. Johns, J. Huang, L. Yu L.X. Chen, T.J. Marks, M.C. Hersam, J. Phys. Chem. Lett. 2 (2011) 3006-3012.

[33] R.Q. Ye, C.S. Xiang, J. Lin, Z.W. Peng, K.W. Huang, Z. Yan N.P. Cook, E.L.G. Samuel, C.C. Hwang, G.D. Ruan, G. Ceriotti, A.R.O. Raji, A.A. Marti, J.M. Tour, Nat. Commun. 4 (2013) 2943.

[34] Y.Q. Dong, C.Q. Chen, X.T. Zheng, L.L. Gao, Z.M. Cui, H. B. Yang, C.X. Guo, Y.W. Chi, C.M. Li, J. Mater. Chem. 22 (2012) 8764-8766.

[35] L. Tian, D. Ghosh, W. Chen, S. Pradhan, X.J. Chang, S.W. Chen, Chem. Mater. 21 (2009) 2803-2809.

[36] D.Y. Pan, J.C. Zhang, Z. Li, M.H. Wu, Adv. Mater. 22 (2010) 734-738.

[37] Y. Li, Y. Hu, Y. Zhao, G.Q. Shi, L.E. Deng, Y.B. Hou, L.T. Qu, Adv. Mater. 23 (2011) 776-780.

[38] Y.Y. Liang, Z. Xu, J.B. Xia, S.T. Tsai, Y. Wu, G. Li, C. Ray L.P. Yu, Adv. Mater. 22 (2010) E135-E138.

[39] N. Blouin, A. Michaud, M. Leclerc, Adv. Mater. 19 (2007) 2295-2300.

Zicheng Ding received his B. S. degree from Wuhan University (China) in 2008 and Ph. D. degree from Changchun Institute of Applied Chemistry (CIAC), Chinese Academy of Sciences (CAS) in 2013. Now he is an assistant professor in Professor Jun Liu's group in State Key Laboratory of Polymer Physics and Chemistry at CIAC. His research is focused on the morphology tuning and device engineering of polymer solar cells.

Zhen Hao received his B. Eng. degree and M. Eng. degree from Hunan University (China) 2010 and 2013, respectively. He works as a research assistant in State Key Laboratory of Polymer Physics and Chemistry at CIAC. His research interest is focused on graphene-related materials and the interface layers of polymer solar cells.

Bin Meng received his B. Eng. degree and M. S. degree in Chemistry from Jilin University (China) in 2004 and 2007, respectively. He is now a Ph. D. candidate at University of Chinese Academy of Sciences. His research is focused on the design and synthesis novel donor polymers for solar cells application.

Zhiyuan Xie received his Ph. D. in solid state electronics and microelectronics from Jilin University (China) in 1999. After a short post-doctoral research at CIAC, CAS, he worked at the City University of Hong Kong as a research associate from 2000 to 2003. He joined Changchun Institute of Applied Chemistry in 2004, and now is a professor of polymer physics and chemistry. His research interest is focused on the organic/polymer optoelectronic devices including solar cells and light-emitting diodes.

Jun Liu received his Ph. D. in Polymer Physics and Chemistry in 2007 from CIAC, CAS. After postdoctoral training at University of Würzburg (Germany), University of California, Los Angeles (USA) and Case Western Reserve University (USA) for five years, he joined CIAC as a principle investigator in 2013. Dr. Liu's research interest includes, design of conjugated polymer materials and graphene materials, and their application in organic photovoltaic devices.

Liming Dai is a Kent Hale Smith Professor in Department of Macromolecular Science and Engineering at Case Western Reserve University. He is also director of the Center of Advanced Science and Engineering for Carbon. Before joining the CWRU, he was an associate professor of polymer engineering at University of Akron and the Wright Brothers Institute Endowed Chair Professor at University of Dayton. He is a Fellow of Royal Society of Chemistry and Fellow of American Institute for Medical and Biological Engineering. His expertise covers the synthesis, functionalization and fabrication of conjugated polymers and carbon nanomaterials for energy- and bio-device applications.